Mehran University Research Journal of Engineering and Technology

https://doi.org/10.22581/muet1982.2302.15

2023, 42(2) 142-150

Effect of variable conduction angle on the losses of switched reluctance machine

Anwar Ahmed Memon [a, *], Ali Asghar Memon [b], Muhammad Aslam Uqaili [b], Mukhtiar Ali Unar [c]

[a] *Institute of Information and Communication Technologies, Mehran University of Engineering and Technology, Jamshoro*

[b] *Department of Electrical Engineering, Mehran University of Engineering and Technology, Jamshoro*

[c] *Department of Computer Systems Engineering, Mehran University of Engineering and Technology, Jamshoro*

[*]Corresponding author: Anwar Ahmed Memon Email: anwar.memon@faculty.muet.edu.pk

Received: 04 February 2023, Accepted: 24 March 2023, Published: 01 April 2023

KEYWORDS

Switched Reluctance Motor

Flux Linkage

Switching Angle

Variable Conduction Angle

ABSTRACT

Switched Reluctance Machine (SRM) is the advanced version of the stepper motor and since last decade, it is of high interest among researchers and industrial applications. Modelling an SRM relies on accurate data and proper selection of parameters. The next step is the performance analysis of the machine for which losses determination is indispensable. Previous studies have shown losses calculation only at a particular instant of switching of the machine (i.e., conduction angle). Therefore, the impact of losses in a motoring region cannot be justified. This paper investigates the impact of varying conduction angle on the performance of machines for a set of switch-on angle. Losses are calculated and predicted through simulating motor operating parameters carried out in MATLAB environment and accuracy of results are compared with experimental results.

1. Introduction

SRM is the advanced version of stepper motor which relies on reluctance torque as opposed to the electromagnetic torque in the traditional motors. The key difference is that the windings are on the stator only while the rotor is made up of laminations. Thus, it is easy to be manufactured and also solves the heating issue. SRMs have also additional benefit of achieving higher power density and speed on same power output. Therefore, it can be used for many applications such as industrial, automation, robotics, etc with greater efficiency. This machine needs a drive circuit and can be operated in variety of speeds and torques. However, due to the non-linearity of the magnetic properties of SRM, it is comparatively difficult to simulate like other motors. The mathematical modelling is mostly performed in software environment (e.g., MATLAB), where the experimental data insertion is not mandatory. The simulation is performed to analyse the efficacy, efficiency, power losses, etc, for various applications, which is then verified/validated with the experimental results. Machine losses are quantified by predicting the losses at fixed or variable conduction angle. In [1], the losses of the machine are predicted on fixed conduction angle [1]. In [2], control of the speed with the control of conduction angle is presented. The converter employed in the drive circuit is half-bridge asymmetrical type where pulse width modulation (PWM) technique is used to control the duty cycle. The comparison of the single switch per phase and half-bridge asymmetrical converter is carried out to conclude the best performance of the machine and the performance of Asymmetrical half-bridge converter is accepted as better in the range of soft switching mode. Furthermore, to enhance the efficiency

and to decrease the torque ripples of the SRM by uncomplicated way of adjusting the switch-on and switch-off angle is presented in [3], in which the small size SR machine is selected in the span of low and high-speed operation. [4] G.J. Li analyzes the performance in terms of flux linkage and inductance per phase and output torque of SRM with new winding configuration called Mutually coupled SRMs. The resulting torque is higher and rippling torque is minimized. M Villani in [5] studies a five-phased SRM for aerospace application which considers it as drive circuit to the electromechanical actuators that can be replace traditional hydraulic and pneumatic actuators. The study involves Finite element method to calculate flux linkages and inductance values for the proper operation. Recently, [6, 10] present an overview of the recent research carried out for SRMs in terms of performance improvement in both design and control circuits. Various research is carried out for the performance evaluation and loss calculation of the SRMs. However, most of the research focuses on technical parameters, torque, losses, conduction angle, and speed. For conduction angle, the performance and losses are evaluated mostly on a fixed conduction angle. This paper on the other hand, focuses on the prediction of losses when the machine is operated in low inductance region for a motoring mode with variable conduction angle. The angle variation is related to the inductance variations, which means that the field is varied and thus the operating parameters may be affected. Additionally, the loss separation method is used to predict the losses by simulating the motor parameters.

The paper is organized as follows: Section 2 briefly explains the modelling of an SRM, Section 3 presents the methodology of the work. The simulation results are given in section 4 while section 5 briefly discusses the results and effect of variable conduction angle on the motor losses and finally section 5 concludes the paper.

2. Modelling an SRM

The mathematical modelling of SRM relies on voltage equation which administers the current through SRM windings, given in Eq. 1 [15, 16]

$$v = Ri + \frac{d\psi}{dt} \tag{1}$$

Where v, R and *i* are the dc voltage supplied (through a suitable converter (drive circuit)), winding resistance and current of the machine respectively, while the second term on the right is the rate of change of flux linkage.

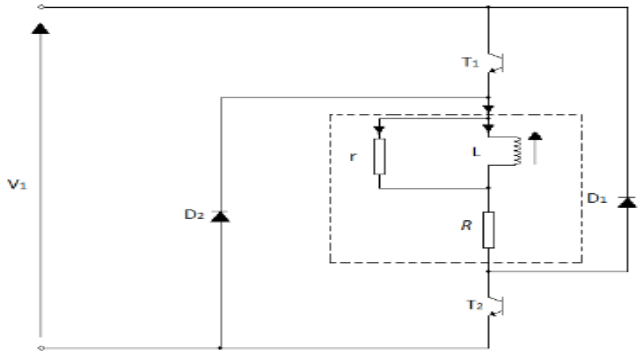

Fig. 1. Equivalent circuit diagram of SRM

An equivalent circuit of SRM is shown in Fig. 1 inspired by [1, 7] in which the procedure of computation of losses in a fixed conduction angle is well addressed. In addition, the diagram of a 4 phase 6/8 pole SRM is shown in Fig. 2. The fixed conduction angle has given a good idea about machine performance leaving a slot for future researchers to find out the behaviour of SRM under variable switch-on and switch-off i.e., variable conduction angle. Two transistors and two diodes are responsible for allowing current to flow through machine winding and provide return path for energy flow back to supply. The data of equivalent iron loss resistance and computation procedure of machine losses is addressed in [1] by including set of equations, given below:

$$I_{rms(ph)} = \sqrt{\frac{1}{T}\int_0^T i^2{}_{ph}\,dt} \tag{2}$$

Where, **T** represents the interval of time, $\boldsymbol{I_{rms(ph)}}$ is the current per phase and $\boldsymbol{i}$ denotes instantaneous current.

The power available at the shaft P_{out}, copper losses $P_{\boldsymbol{cu}}$, and iron losses $P_{\boldsymbol{iron}}$ can be estimated as followed in Eq. 3-5 [14],

$$P_{out} = \omega \times T_{sh} \tag{3}$$

$$P_{cu} = 4I_{rms(ph)}^2 R \tag{4}$$

$$P_{iron\ losses} = P_{input} - \left(P_{out} + P_{cu} + P_{frictional} + P_{conv.loss}\right) \tag{5}$$

Where, ω is the angular velocity, T_{sh} is the shaft torque, while the frictional losses and power convertor losses are denoted by $P_{frictional}$ and $P_{conv.loss}$ respectively.

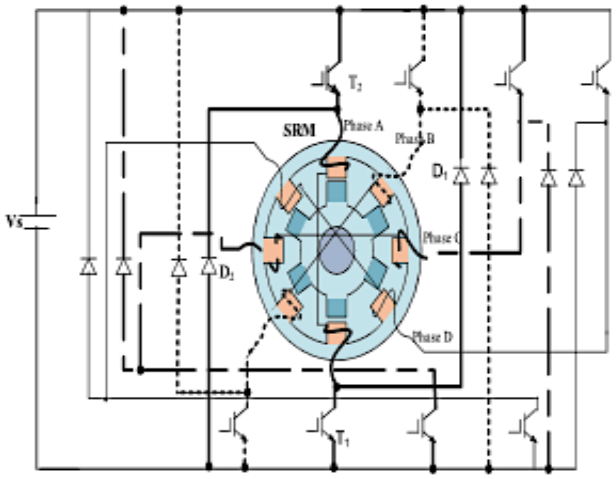

Fig. 2. 8/6 pole construction of SR motor [13]

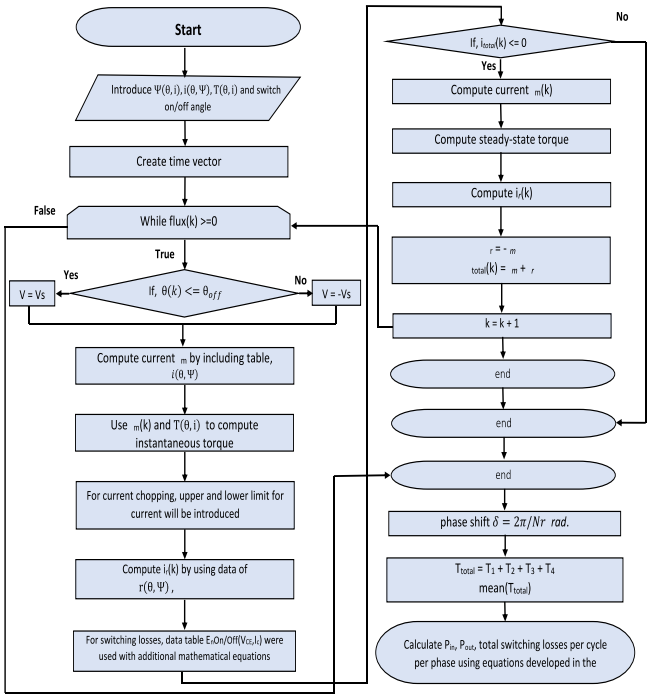

Fig. 3. Flow chart of MATLAB simulation

3. Methodology

In this section, the proposed methodology for predicting the losses of an SRM operating in the motoring region is discusses. Initially, motor parameters are considered, which define operating conditions. Then the conduction angle, defined by the net angles of switch-on and switch-off angles, is changed through control circuit by applying the gate pulse at different switch-on and switch-off angles of the SRM. The data required as input data for the simulation is gathered from the available literature [1, 7] in which fixed conduction angle is considered, specifically the data is taken from [13], where an in-house SRM is implemented. The resulting loss parameters are validated with the designed prototype implemented in the laboratory (see Fig. 6). The correctness of the predicted results through generated model is verified with the previously known experimental outcomes under the fixed conduction angle with same operating conditions and specifications. which confirms the model accuracy. The conduction angle is then varied, for which three cases are considered (see section 4), and the loss parameters for different conduction angles are predicted. Fig.3 shows flowchart [6] of the MATLAB model, created in Simulink, with different operating parameters.

4. Results

The flow chart in the previous section describes the simulation performed to predict the loss parameters at variable conduction angle. Here, we have considered three cases with different conduction angles to estimate/predict the loss parameters. The losses in an SRM occur/reside in three operating regions on any fixed inductance. In this work, low inductance motoring region is considered for the three cases (given below) for both single pulse mode and current chopping mode (different dc pulses) for which the parameters are given in the Table 1.

Case 1: Conduction Angle 30

Case 2: Conduction Angle 31

Case 3: Conduction Angle 25

Table 1

Motor Parameters considered for the three cases

Parameter	Value
Voltage (volts)	100
Speed (RPM)	1311 (Single Pulse) 588 (Current Chopping Mode)
Winding Resistance (Ohm)	3.37
Static Friction (Nm)	0.09
Coefficient of viscous friction (Nm/Rad/Sec)	0.00034
Max. Current	3.2 (Current chopping mode)
Min. Current	3.69 (Current chopping mode)

The SRM is operated when current flows through stator which results in the magnetic field. The drive circuit provides the voltage pulses to excite the pair of the stator windings (in our case 4 pair of stator windings are used because the motor is 8/6 pole), which then creates the variable torque. The flux linkage for different rotor positions is given in Fig. 4. Similarly, the co-

energy is obtained through integrating the flux linkage [12] and is shown in Fig. 5. Co-energy is the function of winding current and the angle Θ in SR machine whereas it is equal to the energy stored in the magnetic field. The static torque is obtained by taking partial derivative of co-energy. The flux and static torque are obtained from [8] and [9] and reconfirmed by designing a prototype shown in Fig. 6 and getting the same data conforming the trend of available data from literature.

In addition to the above parameters, other input conditions include number of switches (8 in this work as a 4-phase SRM is used), 8 free-wheeling diodes, and the instant values of mechanical angle [10] for which the SRM was turned on and then turned off (switch on and off angles).

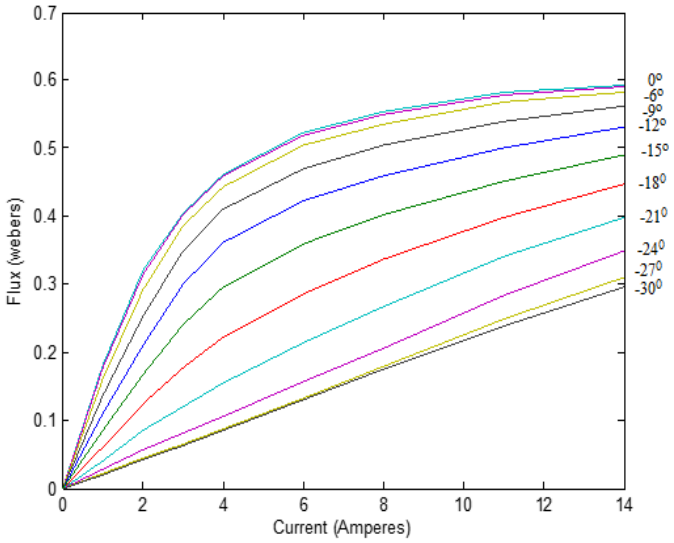

Fig. 4. Flux Linkage characteristics

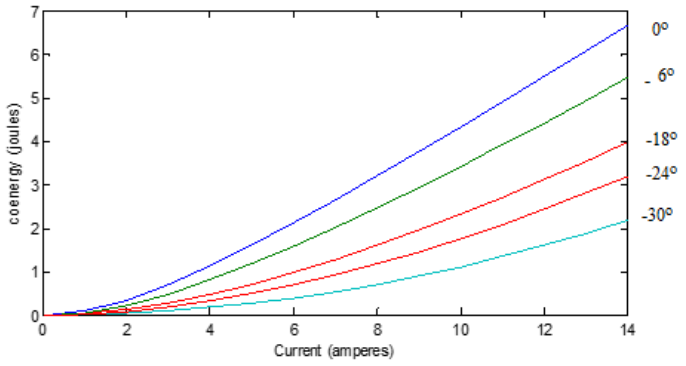

Fig. 5. Co-energy at different values of current

4.1. Case 1: Conduction Angle 30

Conduction angle = 30^0

Switch on Angle: -37^0

Switch Off Angle: $+7^0$

It is noted that the simulation-based results are verified by the practical design/implementation only at 30^0 conduction angle in both the single-pulse and current-chopping modes. The results verify the accuracy of the model and therefore the loss parameters are predicted through simulation model, for other cases.

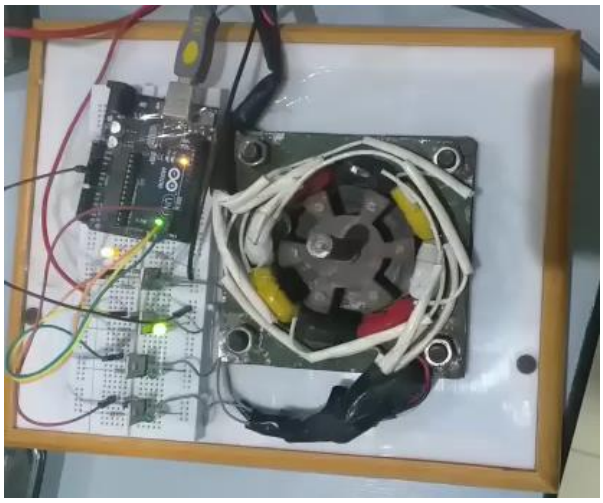

Fig. 6. 8/6 pole SR Motor, its drive and control circuit in operation

In this case, the conduction angle 30^0 is considered for both single pulse and current chopping mode. Since the conduction angle is the net angle of switch on and off angles, the switch on and off angles are -37^0 and $+7^0$ respectively, as shown in the Fig. 7 (single pulse mode) and Fig. 8 (current chopping mode), which show the current curve, which lies only during the conduction region (conduction angle). The dashed line shows the magnetizing current, solid lines show the total current, while the horizontal solid line is the core loss. The resulting loss parameters, for single pulse mode and current chopping mode, are given in the Tables 2 and 3 respectively. It is pertinent to state that the total current in the current chopping mode is less, which is due to the capacitor drawing less current, which offers simple drive circuit, and for this case, reduced speed is considered (see Table 1). The same conditions are used in the implemented motor (Fig. 4), and the copper and iron losses are verified with the predicted results (see Fig. 9) in which the percentage change shows maximum of 5% difference from the actual measured losses, which is satisfactory. Further discussion on the results is given in the next section.

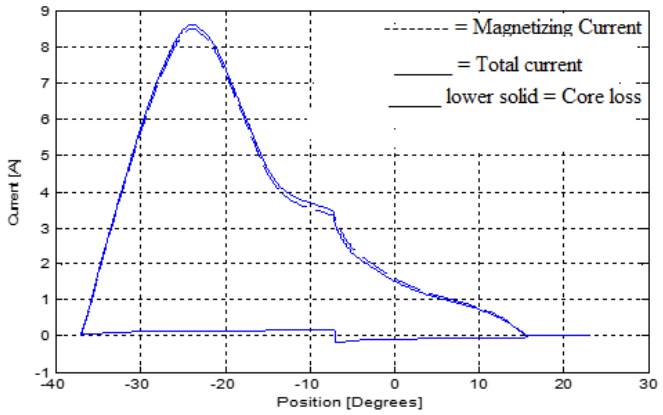

Fig. 7. Representation of current in single pulse mode at 30^0 conduction angle

Table 2

Estimated Loss Parameters at 30 Conduction Angle in Single Pulse Mode

Parameters	Predicted (Simulation based)	Measured (Implemented SRM)	Percentage difference
Input Power	876	870	0.68%
Output Power	543	548	0.92%
Shaft Torque	3.9 Nm	4 Nm	2.50%
Copper Loses	231	243	5.1%
Iron Losses	31.5	32.5	3.17%
Semiconductor Loss	25	24.5	2%

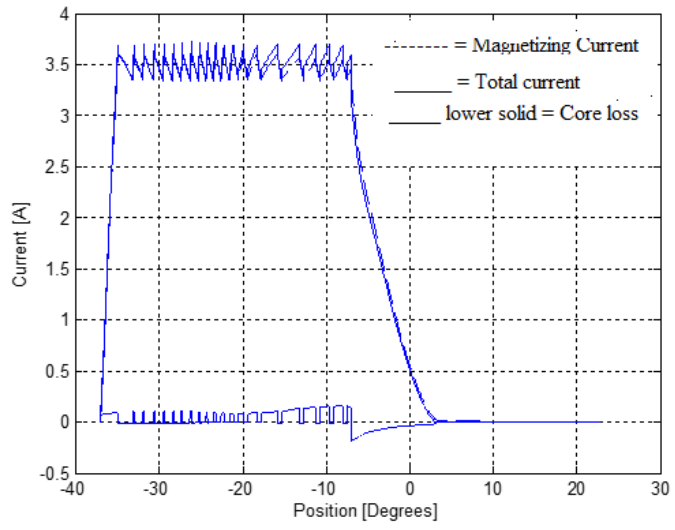

Fig. 8. Representation of current waveforms in current chopping mode at conduction angle of 30 degrees

Table 3

Estimated Loss Parameters at 30^0 Conduction Angle in current chopping mode

Parameters	Predicted (Simulation based)	Measured (Implemented SRM)
Input Power	273	266
Output Power	126.7	123
Shaft Torque	2 Nm	2.8 Nm
Copper Loses	86	93
Iron Losses	15	24.8
Semiconductor Loss	14	13.5

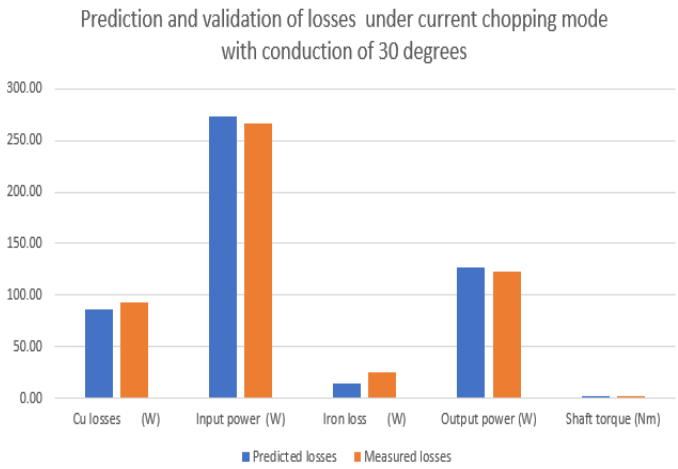

Fig. 9. Production and validation of losses under operating conditions in current-chopping mode at 30^0 conduction angle

4.2 Case 2: Conduction Angle 31^0

Conduction angle = 30^0

Switch-On Angle: -37

Switch-Off Angle: +6

In this case, the conduction angle 31 is considered for both single pulse and current chopping mode, i.e., the switch on and off angles are -37 and +6 respectively, as shown in the Fig. 10 (single pulse mode) and Fig. 11 (current chopping mode), which show the current curve, which lies only during the conduction region (conduction angle). The dashed line shows the magnetizing current, solid lines show the total current, while the horizontal solid line is the core loss. The resulting loss parameters, for single pulse mode and current chopping mode, are given in the Tables 4 and 5 respectively.

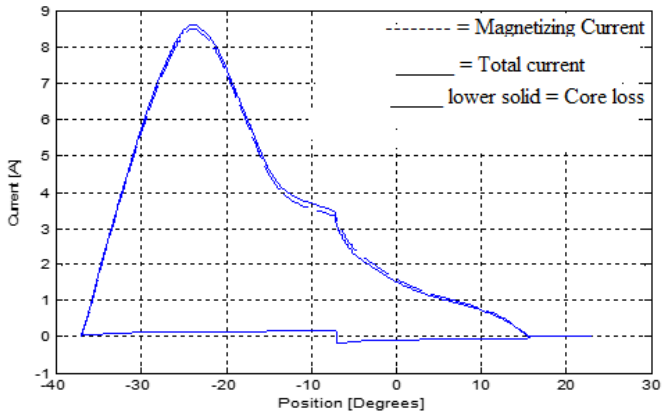

Fig. 10. Representation of current waveforms at conduction angle of 31^0

Table 4

Estimated Loss Parameters at 31^0 Conduction Angle in Single Pulse Mode

Parameters	Predicted (Simulation based)
Input Power	875
Output Power	536.8
Shaft Torque	3.9 Nm
Copper Loses	238
Iron Losses	33.2
Semiconductor Loss	26 W
Friction Loss	18.7 W

Table 5

Estimated Loss Parameters at 31^0 Conduction Angle in Current Chopping Mode

Parameters	Predicted (Simulation based)
Input Power	256
Output Power	126.38
Shaft Torque	2.05 Nm
Copper Loses	83.2
Iron Losses	13.5
Semiconductor Loss	14 W
Friction Loss	6.83 W

4.3 Case 3: Conduction Angle 25^0

Conduction angle = 25^0

Switch on Angle: -30^0

Switch Off Angle: $+5^0$

In this case, the conduction angle 25 is considered for both single pulse and current chopping mode, i.e., the switch on and off angles are -30 and +5 respectively, as shown in the Fig. 12 (single pulse mode) and Fig. 13 (current chopping mode). The dashed line shows the magnetizing current, solid lines show the total current, while the horizontal solid line is the core loss. The resulting loss parameters, for single pulse mode and current chopping mode, are given in the Tables 6 and 7 respectively.

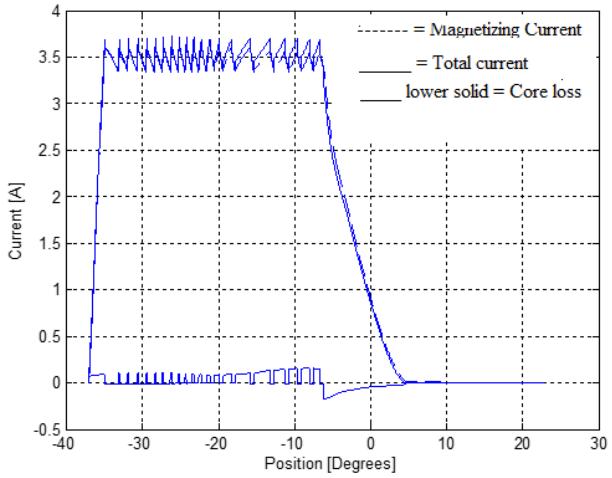

Fig. 11. Representation of current waveforms at conduction angle of 31^0 in current chopping mode

Table 6

Estimated Loss Parameters at 25 Conduction Angle in Single Pulse Mode

Parameters	Predicted (Simulation based)
Input Power	377
Output Power	234
Shaft Torque	1.7 Nm
Copper Loses	69.7
Iron Losses	23
Semiconductor Losses	11.8 W
Friction Losses	18.7 W

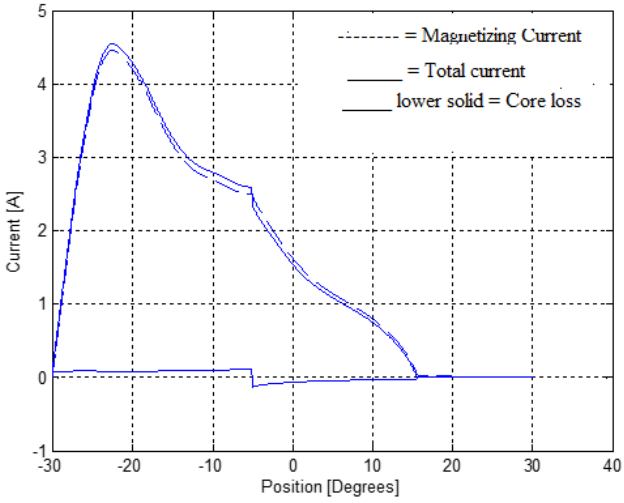

Fig. 12. Representation of current waveforms at conduction angle of 25^0 deg in single-pulse mode

Table 7

Estimated Loss Parameters at 25 Conduction Angle in Current Chopping Mode

Parameters	Predicted (Simulation based)
Input Power	246 W
Output Power	132 W
Shaft Torque	2.14 Nm
Copper Loses	69 W
Iron Losses	13.5 W
Semiconductor Losses	11.59 W
Friction Losses	6.82 W

Table 8

Power Loss Parameters for the three cases with single phase mode

Predicted values	Conduction angle 25^0	Conduction angle 30^0	Conduction angle 31^0
Cu losses (w)	69.7	231	238
input power (w)	377	876	875
iron losses (w)	23	31.5	33.2
output power (w)	234	543	536.8
shaft toque (Nm)	1.7	3.9	3.9
friction loss (w)	15.7	18.6	18.7
Semiconductor losses (w)	11.8	17.4	18.7

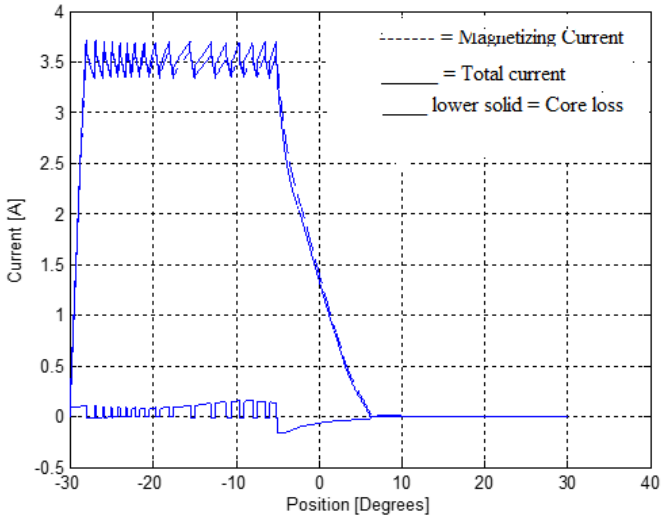

Fig. 13. Representation of current waveforms at conduction angle of 25^0 in current-chopping mode

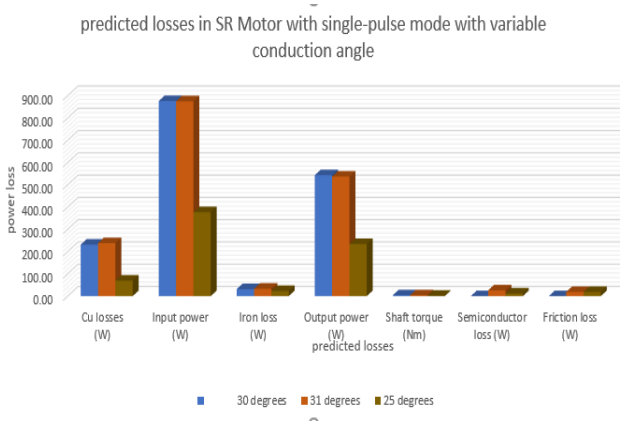

Fig. 14. Predicted losses in single-pulse mode at 25^0, 30^0 and 31^0

5. Discussion

As shown in Fig. 14, conduction angle varies from 25 to 31 degrees. Cu losses are increased when the conduction angle is increased from 25^0 to 31^0 iron loss is increased in the same region of conduction Semiconductor losses have also increased. Since, SRM is a closed loop machine with feedback from the output parameters, load variation forces the motor to send the signals to the control circuit and ultimately the conduction angle will be varied accordingly. The losses will be changing with respect to the conduction angle. Overall, the machine will have more efficiency in running conditions when the energy is being returned to the power supply in de-excitation of the windings.

Fig. 15 shows the comparison of the iron losses at different conduction angles in current chopping mode. As per Table 9, Cu losses increase with the conduction angle because the current increases in the motor windings, but iron losses which depends upon the current density do not increase with conduction angle. At $25^{0,}$ this loss is 13.5 watts, at 30^0, the loss is 18. But the same loss at 31^0 is 13.5. This is because the flux density varies with the phase current, but it also varies with the rotor position.

It is important to highlight that the iron losses are not easy to measure in the practical designs, and since the model predicts the loss parameters with max. 5% difference from the actual practical measurements (as discussed in the Section 4.1). Hence the model can be used for prediction of the loss parameters with different conduction angles, or even different operating parameters.

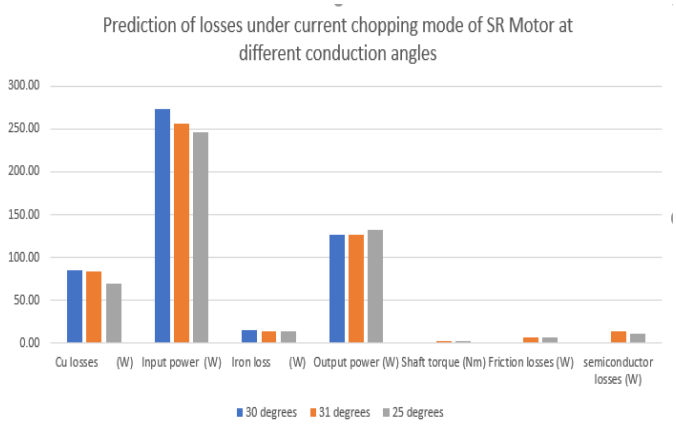

Fig. 15. Losses at different conduction angles in current chopping mode

Table 9

Power Loss Parameters for the three cases with current chopping mode

Predicted values	Conduction angle 25^0	Conduction angle 30^0	Conduction angle 31^0
Predicted Cu losses (w)	69	86	83.2
Predicted input power (w)	246	273	256
Predicted iron losses (w)	13.5	15	13.5
Predicted output power (w)	132	126.7	126.38
Predicted shaft toque (Nm)	2.14	2	2.05
Predicted friction loss (w)	6.82	5.6	6.83
Semiconductor losses (w)	11.59	12.1	14

6. Conclusion

The prediction of SRM losses in a variable conduction angle in MATLAB environment has been presented. The importance of input data and its inclusion in software programming is well addressed. The results obtained with simulations are compared with those obtained through experiments and are justified keeping in view the same operating conditions. Individual losses are evaluated by considering the motor parameters and compared with the measured loss values from the in-house implemented SRM, which shows the 5% variance and since loss calculation is trivial in motoring region [11], the presented work proves the feasibility of the model. The methodology used in this research can be extended in future for different SRM operations (e.g., voltage PWM).

7. Acknowledgment

This research has been performed in the Machines Laboratory, Department of Electrical Engineering, Mehran University of Engineering and Technology, Jamshoro. Authors acknowledge the provision of resources by the administration, which helped us to successfully carry out this research.

8. References

[1] A.A. Memon, S.S.H. Bukhari, and J.S. Ro, "Experimental determination of equivalent iron loss resistance for prediction of iron losses in a switched reluctance machine", IEEE Transactions on Magnetics, vol. 58, no. 2, pp. 1-4, Feb. 2021.

[2] A.A. Memon, “Prediction of losses in a switched reluctance machine and inverter operating with variable conduction angles”, Doctoral dissertation, Department of Electrical Engineering, Mehran University of Engineering and Technology, Jamshoro, Pakistan, 2020.

[3] M. A. Gaafar, A. Abdelmaksoud, M. Orabi, H. Chen and M. Dardeer, "Switched reluctance motor converters for electric vehicles applications: comparative review", IEEE Transactions on Transportation Electrification, 2022.

[4] G.J. Li, X. Ojeda, S. Hlioui, E. Hoang, M. Gabsi and C. Balpe, "Comparative study of Switched Reluctance Motors performances for two current distributions and excitation modes", 35th Annual Conference of IEEE Industrial Electronics, Porto, Portugal, pp. 4047-4052, 2009.

[5] M. Villani, M. Tursini, G. Fabri and L. Di Leonardo, "A switched-reluctance motor for aerospace application", International Conference on Electrical Machines, Berlin, Germany, pp. 2073-2079, 2014.

[6] J.W. Ahn and G.F. Lukman, "Switched reluctance motor: Research trends and overview", CES Transactions on Electrical Machines and Systems, vol. 2, no. 4, pp. 339-347, Dec. 2018.

[7] K. Diao, X. Sun, G. Bramerdorfer, Y. Cai, G. Lei, and L. Chen, “Design optimization of switched reluctance machines for performance and reliability enhancements: A review”,

Renewable and Sustainable Energy Reviews, vol. 168, p.112785, 2022.

[8] Sherla, B. Pramesh, H. Gupta, J. Thite, and R. Jayapragash, "Conduction Angle Control of Switched Reluctance Motor", Journal of Physics: Conference Series, vol. 1716, no. 1, p. 012011. IOP Publishing, 2020.

[9] Bober, Peter, and Želmíra Ferková, "Firing angle adjustment for switched reluctance motor efficiency increasing based on measured and simulated data", Electrical Engineering, vol. 104, no. 1, pp. 191-202, ,2022.

[10] Xu, Zhenyao, Tao Li, Fengge Zhang, Yue Zhang, Dong-Hee Lee, and Jin-Woo Ahn. "A review on segmented switched reluctance motors", Energies, vol. 15, no. 23, p. 9212, 2022.

[11] A.A. Memon, M.M. Shaikh, S.S.H. Bukhari, and J.S. Ro, "Look-up data tables-based modeling of switched reluctance machine and experimental validation of the static torque with statistical analysis", Journal of Magnetics, vol. 25, no. 2, pp. 233-244, 2020.

[12] A.A. Memon, A.A. Memon, M.A. Uqaili, and M.A. Unar, “Modeling of flux linkage characteristics of switched reluctance motor”, Indian Journal of Science and Technology, vol. 12, p.17, 2019.

[13] A.A. Memon, and M.M. Shaikh, "Input data for mathematical modeling and numerical simulation of switched reluctance machines", Data in brief, vol. 14, pp. 138-142, 2017.

[14] L. Chen, H. Chen, and W. Yan, “A fast iron loss calculation model for switched reluctance motors”, IET Electric Power Applications, vol. 11, no. 3, pp. 478-486, 2017.

[15] A.A. Memon, S.A.A. Shah, W. Shah, M.H. Baloch, G.S. Kaloi, and N.H. Mirjat, "A flexible mathematical model for dissimilar operating modes of a switched reluctance machine", IEEE Access, vol. 6, pp. 9643-9649, 2018.

[16] J. Corda and S.M. Jamil, "Experimental determination of equivalent-circuit parameters of a tubular switched reluctance machine with solid-steel magnetic core", IEEE Transactions on Industrial Electronics, vol. 57, no. 1, pp. 304-310, Jan. 2010.

